



Fibroblast growth factor 10 regulates Meckel's cartilage formation during early mandibular morphogenesis in rats

Fumie Terao^a, Ichiro Takahashi^{a,e}, Hidetoshi Mitani^a, Naoto Haruyama^{b,f}, Yasuyuki Sasano^c, Osamu Suzuki^d, Teruko Takano-Yamamoto^{a,*}

^a Division of Orthodontics and Dentofacial Orthopedics, Tohoku University Graduate School of Dentistry, 4-1 Seiryomachi, Aoba-ku, Sendai 980-8575, Japan

^b Division of Oral Dysfunction Science, Tohoku University Graduate School of Dentistry, 4-1 Seiryomachi, Aoba-ku, Sendai 980-8575, Japan

^c Division of Craniofacial Development and Regeneration, Tohoku University Graduate School of Dentistry, 4-1 Seiryomachi, Aoba-ku, Sendai 980-8575, Japan

^d Division of Craniofacial Function Engineering, Tohoku University Graduate School of Dentistry, 4-1 Seiryomachi, Aoba-ku, Sendai 980-8575, Japan

^e Division of Oral Health, Growth and Development, Section of Orthodontics and Dentofacial Orthopedics, Kyushu University Faculty of Dental Science, 3-1-1 Maidashi, Higashi-ku Fukuoka, 812-8582, Japan

^f Global Center of Excellence Program, International Research Center for Molecular Science in Tooth and Bone Disease, Tokyo Medical and Dental University, 1-5-45 Yushima, Bunkyo-ku Tokyo 113-8549, Japan

ARTICLE INFO

Article history:

Received for publication 23 June 2010

Revised 18 October 2010

Accepted 29 November 2010

Available online 11 December 2010

Keywords:

Rat embryo

FGF10

Sox9

Col2a1

Chondrogenesis

Meckel's cartilage

Electroporation

Gene transfer

Mandibular organ culture

ERK

Phosphorylation

ABSTRACT

Fibroblast growth factors (FGF) are pluripotent growth factors that play pivotal roles in the development of various organs. During mandibular organogenesis, Meckel's cartilage, teeth, and mandibular bone differentiate under the control of various FGF. In the present study, we evaluated the role of FGF10 in rat mandibular chondrogenesis and morphogenesis using mandibular organ culture and mandibular cell micromass culture systems. The overexpression of *Fgf10* induced by the electroporation of an FGF10 expression vector not only altered the size and shape of Meckel's cartilage, but also upregulated the expression of the cartilage characteristic genes *Col2a1* and *Sox9* in a mandibular organ culture system. Meckel's cartilage was deformed, and its size was increased when *Fgf10* was overexpressed in the lateral area of the mandible. Meanwhile, no effect was found when *Fgf10* was overexpressed in the medial portion. In the mandibular cell micromass culture, recombinant FGF10 treatment enhanced chondrogenic differentiation and endogenous ERK (extracellular signal-regulated kinase) phosphorylation in cells derived from the lateral area of the mandible. On the other hand, FGF10 did not have significant effects on mandibular cell proliferation. These results indicate that FGF10 regulates Meckel's cartilage formation during early mandibular morphogenesis by controlling the cell differentiation in the lateral area of the mandibular process in rats.

© 2010 Elsevier Inc. All rights reserved.

Introduction

Craniofacial embryonic development is regulated by complex three-dimensional cell–cell and cell–epigenetic factor interactions (Chai et al., 1998; Cobourne and Sharpe, 2003; Ferguson et al., 2000; Slavkin et al., 1990). Mandibular morphogenesis starts with the migration of cranial neural crest cells (CNCC) to the branchial arches and the formation of Meckel's cartilage (Chai et al., 2000) in the mandibular process. It is known that the disharmony of the migration of CNCC or the factors, which control the pattern formation and morphogenesis during embryonic development in the facial primordia, gives rise to the craniofacial malformation or mandibular deformity. During Meckel's cartilage morphogenesis, chondrogenesis progresses via mesenchymal proliferation and the differentiation of

chondrocytes similar to the processes involved in the development of other skeletal elements. These steps are regulated by the growth factors described below and transcription factors such as Sox-5, 6, and 9, which results in the expression of type II collagen, Aggrecan, and type X collagen (Bi et al., 1999; Silbermann and von der Mark, 1990).

Crouson, Phifer and Apert syndromes have been known to be caused by the mutations in fibroblast growth factor receptors, of which alteration of signal intensity by mutation in the extracellular domain of the receptors lead their characteristic phenotype; craniosynostosis. In these syndromes, it has been suggested that facial morphology is affected to be prognathic due to the impaired growth balance of maxillary and mandibular bones could be affected. Fibroblast growth factors (FGF) are known to regulate cell-fate specification and determination, and branching morphogenesis in many contexts during mammalian organogenesis through the extracellular-signal-regulated kinase (ERK) mitogen-activated protein kinase (MAPK) pathway (Steinberg et al., 2005; Unbekandt et al., 2008). FGF10 and FGF8 play crucial roles in limb development by inducing cell

* Corresponding author. Fax: +81 22 717 8372.

E-mail address: t-yamamo@tohoku.ac.jp (T. Takano-Yamamoto).

proliferation, cell-fate specification, and cytodifferentiation during limb cartilage development and growth (Lewandoski et al., 2000). They reciprocally stimulate their own expression in the mesenchyme and epithelium in order to induce the outgrowth of limb buds and progressive pattern formation in limb buds (Ohuchi et al., 1997). Those reciprocal stimulations are transferred to each other through FGFRs expressed in the mesenchyme and KGFR; alternative spliced form of FGFR2 specifically expressed in epithelium. Similarly, FGF10 and FGF8 are expressed in mandibular mesenchymal and epithelial cells, respectively, which play critical roles in tooth and mandibular bone development (Ferguson et al., 2000; Havens et al., 2006; Mina, 2001). Indeed, in tooth development, FGF8 expressed in the epithelial dental lamina and BMP2 and 4 coordinately contributes to cell-fate determination in the tooth mesenchyme (Neubüser et al., 1997). In addition, epithelial FGF8 has been indicated to be involved in pattern formation in the mandible (Shigetani et al., 2000); however, the functions of FGF10 and its receptor in mandibular morphogenesis have not been clarified yet.

In the present study, we hypothesized that FGF10 enhances chondrogenic differentiation in the mandibular mesenchyme and increases the length of Meckel's cartilage.

To test this hypothesis, we first attempted to verify the roles of FGF10 in the control of the shape and size of the Meckel's cartilage formed during mandibular morphogenesis by electroporating an FGF10 expression vector into a mandibular organ culture system. We also examined the role of FGF10 in rat mandibular chondrogenesis

and morphogenesis using a mandibular cell micromass culture system. Here, we demonstrate that the time- and region-specific expression of FGF10 regulates chondrogenesis via ERK phosphorylation in developing mandibular processes.

Materials and methods

Experimental animals

Timed pregnant Sprague–Dawley rats were used on gestation day 12 (E12) (with the day when the vaginal sperm plug was first observed designated as day 0 of gestation). The mandibular processes of E12 embryos were microdissected in ice-cold phosphate-buffered saline (PBS) at pH 7.4 and subsequently washed in cold PBS (Fig. 1A; Md). All protocols for the animal experiments were reviewed and approved by the Animal Care and Use Committee of Tohoku University.

Organ culture

The E12 rat mandibular processes were cultured on a Millipore membrane in serum-free chemically-defined BGJb medium (Invitrogen, CA, USA) supplemented with 100 U of penicillin and streptomycin (Invitrogen) and 100 µg/ml L-ascorbic acid (Sigma, MO, USA) in 5% CO₂ at 37 °C, as demonstrated previously (Nonaka et al., 1999; Semba et al., 2000; Yamane et al., 2003). They were then preincubated for 3 h prior to

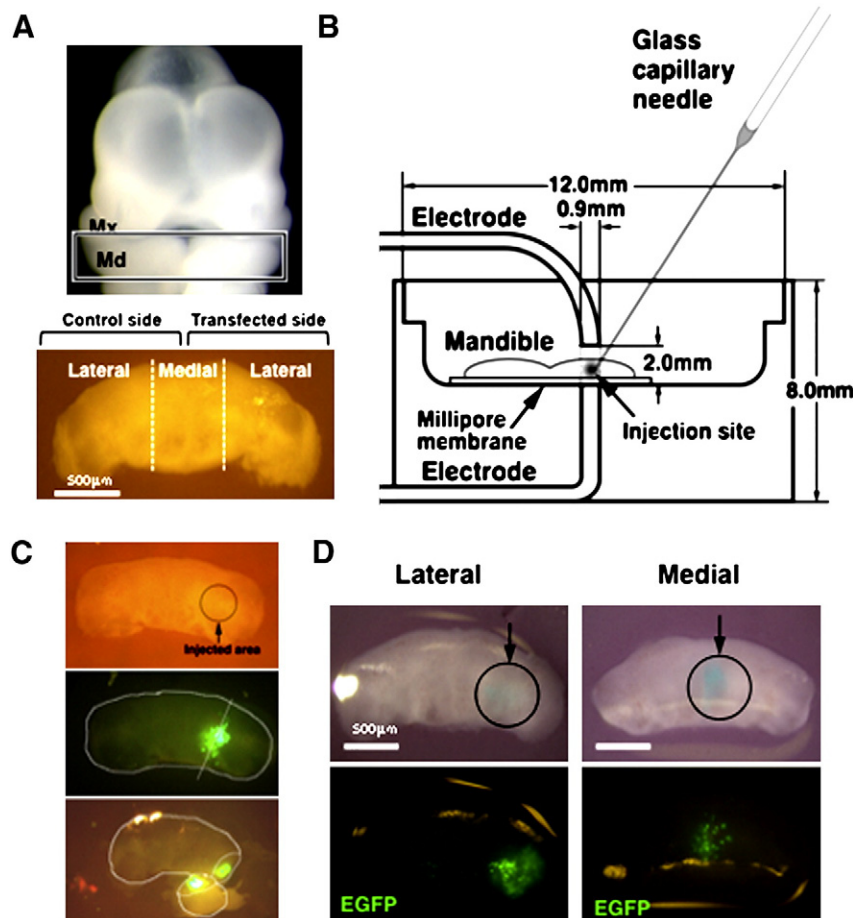


Fig. 1. Experimental procedures and schematic illustration of gene transfection. (A) Craniofacial region of an E12 rat embryo and a mandibular explant dissected and cultured for 3 h. The boxed mandibular process was dissected for further analysis. Mx: Maxillary process, Md: Mandibular process. Bars = 500 µm. Dotted lines indicate the borders between the lateral and medial areas defined in the present study. (B) Schematic illustration of the electroporation apparatus, showing the mandible and the glass capillary needle used for microinjection. (C) Mandibular organ culture samples 24 h after electroporation. The circles indicate the areas into which the EGFP expression vector was microinjected. Restricted EGFP gene expression was detected in the lateral or medial region of the transfected side of each mandible. (D) Transfection of the EGFP expression vector to lateral or medial region of the mandibular explant. The circles indicate the areas into which the EGFP expression vector was microinjected.

electroporation or initial whole mount *in situ* hybridization analysis. After the electroporation, the mandibular processes were cultured for 7 days.

Generation of the cRNA probes for *in situ* hybridization analysis

cDNA fragments for *Sox9*, *Col2a1*, *Aggrecan*, *Fgf10*, and *Fgfr1* to 3 were obtained by the reverse transcription (SuperScript II RT kit, Invitrogen) -polymerase chain reaction (RT-PCR) from a total RNA sample prepared from a rat E13 embryo. The primers, which were designed based on rat cDNA sequences, and the PCR conditions used are indicated in Table 1. The obtained cDNA fragments were then subcloned into the pCRITOPPO vector (Invitrogen) according to the manufacturer's instructions and sequenced (Hokkaido System Science, Sapporo, Japan). To create digoxigenin (DIG) -labeled riboprobes (Roche Diagnostics, IN, USA) for the sense and antisense fragments, the plasmids were linearized by restriction enzymes and transcribed using Sp6, T7, or T3 (Invitrogen) into cRNA, as indicated in Table 1.

Whole-mount *in situ* hybridization

Whole-mount *in situ* hybridization was performed as previously described (Rosen and Beddington, 1993) at 0 (+3 h) or 1 day of mandibular organ culture. The specimens were then fixed overnight in 4% PFA in PBS at 4 °C, bleached using 6% hydrogen peroxide in PBS supplemented with 0.1% Tween 20 at room temperature, and permeabilized with 10 µg/ml proteinase K (Roche Diagnostics) for 10–20 min at room temperature. Post-fixation and prehybridization, the specimens were hybridized with 1–2 µg/ml of the DIG labeled riboprobes at 70 °C overnight. Non-specific immuno-reactions were blocked with 10% normal sheep serum (Sigma), and then the specimens were incubated with anti-DIG alkaline phosphatase-conjugated antibody (Roche Diagnostics) overnight at 4 °C. The color reaction was developed using nitro blue tetrazolium (NBT) and 5-bromo-4-chloro-3-indolyl phosphate (BCIP) as substrates (Roche Diagnostics).

FGF10 plasmid construction, microinjection, and gene transfer

The coding sequence of rat *Fgf10* (GenBank accession #: NM_012951) was amplified by PCR with Pfx (Invitrogen) DNA polymerase from the E13 rat cDNA using the primers indicated in Table 1. Upstream primers harboring an XhoI site and downstream primers harboring an EcoRI site were used for cloning. The obtained fragments were subcloned into the multicloning site of the pCRITOPPO vector (Invitrogen) and sequenced (Hokkaido System Science). After no mutations in the sequences in the FGF10 gene were confirmed, the

fragments were excised by XhoI and EcoRI and inserted into a vector with a pCMS-EGFP mammalian expression plasmid vector (Clontech, La Jolla, CA) backbone, which we constructed previously (Terao et al., 2007).

The protocol for electroporation of the plasmid into the mandibular organ culture system was also demonstrated in our previous study (Terao et al., 2007). Briefly, DNA solutions containing the FGF10 expression vector or EGFP (Mock) vector were labeled with 0.05% Fast Green solution (Sigma) and injected into mandibular explants using a micromanipulator and a microinjector (Narishige, Tokyo, Japan) with a glass capillary needle prior to electroporation. The amount injected was monitored, and it was determined under microscopic observation that the diameter of the green spot produced by microinjection was one third of the anteroposterior width of the explant. The gene solution was microinjected into the right side of the lateral or medial section of the mandibular explant (Fig. 1B). Custom-made platinum electrodes of 0.9 mm in diameter placed 2.0 mm apart were prepared for the present study (Fig. 1C). Four 20 V square pulses with a duration of 50 ms and a 100 ms inter-pulse interval were produced in physiological saline using an electroporator (CUY-21, Nepa gene, Chiba, Japan). At 24 h after transfection, the EGFP protein in the living explants was observed under a fluorescent microscope and EGFP was expressed intensely in the mesenchyme on cross-sections of the explant, (Fig. 1D). EGFP expression was observed in medial and lateral section of the explant respectively (Fig. 1E).

The constructed FGF10 expression vector was also transfected into COS-7 cells, which were provided by the Cell Resource Center for Biomedical Research Institute of Development, Aging, and Cancer at Tohoku University (Sendai, Japan) using FuGENE HD (Roche Diagnostics), according to the manufacturer's protocol.

Whole-mount Alcian blue staining and measurement of cartilage length in mandibular explants

Whole-mount Alcian blue staining was performed at 1, 3, 4, and 7 days of mandibular explant organ culture. The explants were incubated with 0.5% Alcian blue 8GX (Sigma) in 95% acidic ethanol overnight and cleared in 0.1 M potassium hydroxide. For the measurement of cartilage length, the Alcian blue-stained samples were dehydrated and embedded in paraffin, and 5-µm-thick horizontal sections were cut for three-dimensional reconstruction of Meckel's cartilage. The images of the sections were digitized using a CCD camera, and Alcian blue-positive areas of all sections were converted to binary images using Photoshop (Adobe, CA, USA). Computer-assisted three-dimensional (3D) reconstructions were created using Imaris 4 (Carl Zeiss, Jena, Germany). We resliced the 3D images frontally into 5 µm-thick slices and measured the length of Meckel's cartilage from the constriction between the triangular portion in the

Table 1
Conditions for cloning, creating riboprobes, and semi-quantitative RT-PCR.

| Gene name | GenBank accession No. | Nucleic acid sequences of primers | | Product size | Restriction enzymes for RNA polymerase | | | PCR annealing temperature (°C) | Cycle |
|-----------|-----------------------|-----------------------------------|-------------------------|--------------|--|-----|-------|--------------------------------|-------|
| Sox9 | AB073720 | Upstream | AAGAAGGAGAGCGAAGAAGATAA | 339 | Anti-sense | T3 | BamHI | 58 | 24 |
| | | Downstream | CTTGTAATCGGGGTGGTCTTT | | Sense | T7 | Apal | | |
| Col2a1 | L48440 | Upstream | GTGAGAGCGGAGAC | 665 | Anti-sense | T7 | BamHI | 55 | 24 |
| | | Downstream | TAGAGTGACTGGGGTTAGA | | Sense | Sp6 | XhoI | | |
| Fgf10 | NM_012951 | Upstream | AAGAACGGCAAGGTCAGC | 328 | Anti-sense | T7 | BamHI | 60 | 28 |
| | | Downstream | GAGGAAGTGAGCGGAGGTG | | Sense | Sp6 | XhoI | | |
| Fgfr1 | NM_024146 | Upstream | CTACCGCCACAAGACC | 941 | Anti-sense | Sp6 | XhoI | – | – |
| | | Downstream | TGCAGATACTCCCCAAGA | | Sense | T7 | SpeI | | |
| Fgfr2 | XM_341940 | Upstream | GGCCCTCCTTCAGTTTAG | 650 | Anti-sense | Sp6 | XhoI | – | – |
| | | Downstream | CCCGTATTCAITCTCCAC | | Sense | T7 | SpeI | | |
| Fgfr3 | AF277717 | Upstream | CGCACAGCCACACATCC | 705 | Anti-sense | T7 | SpeI | – | – |
| | | Downstream | GTCGCATCATCTTTCAGCAT | | Sense | Sp6 | XhoI | | |
| GAPDH | NM_017008 | Upstream | TGTTTGTGATGGGTGTGAA | 485 | – | – | – | 55 | 24 |
| | | Downstream | ATGGGAGTTGCTGTTGAAG | | – | – | – | | |

central section and rods to the curvature at the border between the rods and ear cartilage by tracing the centers of the cartilage rod sections.

Tissue preparation for histological examination and in situ hybridization

After the mandibular explants had been cultivated with daily changes of the medium for the indicated experimental periods, they were fixed with 4% paraformaldehyde (PFA) and 0.5% glutaraldehyde in 0.1 M PBS for 30 min at 4 °C. Then, the specimens were dehydrated in a graded series of ethanol and embedded in paraffin. Five μ m-thick horizontal sections were cut for histological examinations and *in situ* hybridization. For regular histological observations, sections were stained with hematoxylin and eosin (H & E).

The *in situ* hybridization protocol used in the present study was described in previous studies (Ohtani et al., 1992; Sasano et al., 1996; Zhu et al., 2001). Briefly, the sections were deparaffinized, rehydrated, and immersed in 0.2 N HCl for 20 min at room temperature and then incubated with 20 μ g/ml proteinase K (Roche Diagnostics) at 37 °C for 30 min. After the sections had been dehydrated in ethanol, they were hybridized with approximately 400 ng/ml of the DIG-labeled riboprobes at 45 °C for 16 h, before being incubated with 20 μ g/ml RNase A (Sigma) in 1 \times SSC (saline-sodium citrate buffer) and then thoroughly washed in 2 \times SSC and 1 \times SSC at 45 °C. After the sections had been incubated with anti-DIG alkaline phosphatase-conjugated antibody (Roche Diagnostics) at 4 °C overnight in a moisture chamber, signals were visualized using NBT and BCIP as substrates (Roche Diagnostics). Nuclear counterstaining was performed using 0.5% methyl green. The sections were mounted and observed under light microscopy.

Mandibular cell micromass culture

The E12 rat mandibular processes were divided into medial and lateral regions of both sides of the mandible at the most prominent portion of the mandibular process in the horizontal plane where the dotted line is indicated in Fig. 1A (Mina, 2001) in ice-cold PBS and then were treated in 0.25% trypsin EDTA and 0.25 mg/ml collagenase type 2 (Invitrogen, Carlsbad, CA) in 0.1 M PBS for 10 min at 37 °C and then dissociated into single cell suspensions. The cells were resuspended in Dulbecco's modified Eagle's medium (DMEM) (Invitrogen) at a density of 2×10^7 cells/ml, and one 20 μ l drop was plated on a 24-well culture plate (Greiner Bio-one, Frickenhausen, Germany) and maintained for 3 h in a incubator at 37 °C and 5% CO₂ to permit cell attachment. Subsequently, 1 ml of DMEM supplemented with 10% heat-inactivated fetal bovine serum (JRH Bioscience, Lanexa, KS), 2.4 mg/ml N-(2-hydroxyethyl) piperazine-N'-(ethanesulfonic acid) (HEPES) (Dojindo Molecular Technologies Inc., Kumamoto, Japan), 0.2% sodium bicarbonate (Sigma), and 100 U each of penicillin and streptomycin (Invitrogen) were added.

After 1 day of incubation, the medium was replaced with medium consisting of various concentrations (0 ng/ml for a control group; 1, 5, or 25 ng/ml for the experimental groups) of recombinant human FGF10 (rhFGF10, R&D Systems, Minneapolis, MN, USA). After being cultured for 3 days, the experimental groups treated with rhFGF10 were divided into two groups, the (++) group, which was cultured with rhFGF10 protein throughout the experimental period, and the (+−) group, which was cultured with rhFGF10 alone for the first 3 days and released from rhFGF10 treatment thereafter so that the initial effect of rhFGF10 treatment could be examined. The culture medium was replaced every other day.

After 7 days of culture, the cells were fixed with 2% acetic acid in 95% ethanol for 15 min at room temperature, rehydrated, and stained overnight at 4 °C with 0.5% Alcian Blue 8GX (Sigma) in 0.1N HCl. The cultures of all groups were microphotographed using a digital camera (Coolpix 955, Nikon, Tokyo, Japan), and then the area of Alcian blue-positive nodules was measured.

Semi-quantitative RT-PCR analysis

After the explants had been incubated for each experimental period, total RNA was extracted using a total RNA isolation kit (RNeasy mini kit, Qiagen). The adjusted amount of total RNA was reverse transcribed into cDNA using a SuperScript II reverse transcription kit (Invitrogen). To avoid contamination of the plasmid DNA, total RNA samples were treated with DNase I (Roche Diagnostics) under RNase-free conditions for 1 h at 37 °C prior to reverse transcription. PCR was performed for glyceraldehyde-3-phosphate dehydrogenase (*GAPDH*), *Fgf10*, *Sox9*, and *Col2a1*. PCR amplification was carried out using recombinant Taq polymerase (Invitrogen) and a PTC-100 programmable thermal controller (MJ Research, MA, USA). The thermal cycling program for semi-quantitative PCR consisted of 4 min and 15 s of predenaturation at 95 °C and various numbers of cycles of 45 s for denaturation, 45 s of annealing at the optimized temperature, and 2 min of extension at 72 °C, followed by a final extension cycle of 10 min. The nucleic acid sequences of the primers, the PCR conditions such as the number of cycles, and the accession number of each gene are shown in Table 1. The expression levels of each gene were normalized against *GAPDH*. The PCR products were electrophoresed, stained with ethidium bromide, and digitized using a CCD camera. The optical density of the bands was quantitated using Image J software (NIH).

Western blotting analysis

Protein accumulation of phosphorylated ERK in the micromass culture was analyzed using Western blotting analysis. Cells from 4 wells were lysed in a buffer containing 50 mM Tris base-HCl (pH 8.0), 150 mM NaCl, 0.5% Triton-X, 1 μ g/ml leupeptin, 5 μ g/ml aprotinin, 0.5 mM phenylmethylsulfonylfluoride (PMSF), 1 mM EDTA, 1 mM EGTA, 1 mM Na₃VO₄, 1 mM NaF, and 10 mM sodium pyrophosphate (all reagents from Sigma) at 3 days of culture. The concentration of protein was measured using a Micro BCA protein assay reagent kit (Pierce Biotechnology, IL, USA), and then 30 μ g of protein were subjected to further analysis.

To verify that the expression vector was expressing FGF10 protein, the COS-7 cell culture supernatant and lysate were collected at two days after transfection. The supernatant was concentrated with a membrane filter unit (Microcon, Millipore Corp., MA, USA) before the sample preparation.

The proteins produced were separated by sodium dodecylsulfate-polyacrylamide gel electrophoresis (SDS-PAGE) on 12.5% gels (Atto, Tokyo, Japan) according to the manufacturer's instructions and then transferred to nitrocellulose membranes (Bio-Rad Laboratories, CA, USA). ERK was detected using polyclonal antibody 9101 against p44/42 MAP kinases (Erk1/2) and antibody 9102 against phosphorylated p44/42 MAP kinases (Cell Signaling Technology, MA, USA). The production of FGF10 protein was confirmed using rabbit anti-FGF10 polyclonal antibody (H-121: sc-7917; Santa Cruz Biotechnology, CA, USA) at a 1:200 dilution. The primary antibodies were detected using goat anti-rabbit IgG antibody conjugated to horseradish peroxidase (Cell Signaling Technology) and the SuperSignal West Pico chemiluminescent substrate (Pierce Biotechnology Inc., IL, USA) as per the manufacturer's instructions.

Cell proliferation assay in mandibular cell cultures

The cell proliferation occurring in the mandibular cell monolayer culture was evaluated using Cell Counting Kit-8 (Dojindo Molecular Technologies, Inc). Cultures of mandibular cells were plated in 96-well plates at 1.0×10^4 cells per well and treated with 0, 1, 5, or 25 ng/ml rhFGF10 for 3 days. After the addition of the cell counting reagent (WST-1), the cells were incubated at 37 °C for 4 h. Absorbance was

measured at a wavelength of 450 nm using a Tecan Sunrise remote microplate reader (Tecan, Austria).

Statistical analysis

The length of Meckel's cartilage was analyzed using the paired t-test. The quantitative data for Sox9 and Col2a1 gene expression and Alcian blue staining were subjected to statistical analysis using two-way factorial ANOVA followed by Tukey's post hoc analysis. The data from the Western blotting and the proliferation assay supplemented with rhFGF10 were analyzed by one-way ANOVA test and Tukey's post hoc comparison. *P* values <0.05 were considered statistically significant.

Results

Endogenous expression pattern of *Fgf10*, chondrogenic markers, and *Fgfr*

Whole mount *in situ* hybridization was carried out after 3 h or 1 day of culture to determine the normal expression patterns of *Fgf10* and chondrogenic marker genes before transfection of the *Fgf10* expression vector (Figs. 2A–F). Endogenous *Fgf10* was weakly expressed throughout the mesenchyme of the mandibular explants at Day 0 + 3 h (Fig. 2A), and the expression pattern became more

restricted to the oral side of the mandible just inside of the Meckel's cartilage in the mesenchyme (Fig. 2B). Sox9 expression was weakly detected in the region of the future Meckel's cartilage (Fig. 2C), but its expression was clearly detected at day 1 (Fig. 2D). Col2a1 expression was also detected in the region corresponding to the future Meckel's cartilage (Fig. 2F).

The expression of FGF receptors was recognized at Day 0 + 3 h and Day 1 in the mandibular explants (Figs. 2G–L). After cultivation for a day, *Fgfr1* expression was observed in the anterior proximal region of the mandibular explants and the area of future Meckel's cartilage (Fig. 2G), and *Fgfr2* was expressed in the anterior-most area of the mandible as well as the posterior region where the tongue is formed (Figs. 2I and J). The weak expression of *Fgfr3* was detected in the mandible at Day 0 + 3 h and Day 1 (Figs. 2K and L). The expression of *Fgfr1* and *Fgfr2* was overwrapped in the medial anterior proximal area of the mandibular process while the expression domain of *Fgfr1* extended to the lateral area at day 1. This lateral domain of *Fgfr1* gene expression co-localized with the expression of Sox9 or Col2a1 at day 1. *Fgf10* gene seemed to be expressed in immediate inside of the area where Sox9, Col2a1 and *Fgfr1* were expressed at the border between medial and lateral part of mandible. On the one hand, *Fgfr2* showed no clear correlation with any other genes examined in the present study. *Fgfr3* expression area covered whole mandibular process overwrapping with other *Fgfrs*.

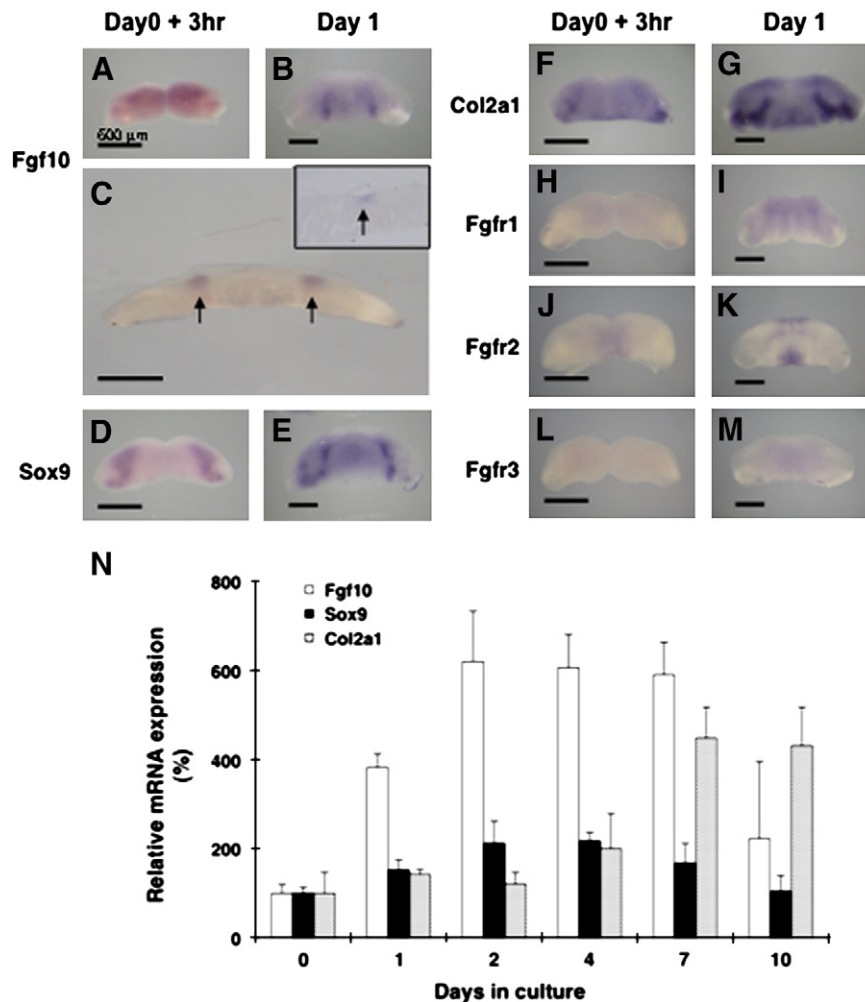


Fig. 2. Gene expression of *Fgf10*, Sox9, Col2a1, and *Fgfr* receptors on Day 0 + 3 h or Day 1 of organ culture. The *Fgf10* (A and B), Sox9 (C and D), Col2a1 (E and F), *Fgfr1* (G and H), *Fgfr2* (I and J), and *Fgfr3* (K and L) gene expression patterns in mandibular explants were examined by whole mount *in situ* hybridization at Day 0 + 3 h (A, C, E, G, I, and K) and 1 day (B, D, F, H, J, and L) after the beginning of organ culture. Bars = 500 μm. (M) The amounts of *Fgf10*, Sox9, and Col2a1 mRNA expressed were measured using semi-quantitative RT-PCR analysis at different time points. The results are expressed as the mean ± SD (N = 3 in each group). The expression of *Fgf10* peaked on day 2 of culture, and its expression level was maintained until day 10. The expression of Sox9 showed a similar pattern to *Fgf10*, while it was decreased by day 10. Col2a1 expression gradually increased throughout the culture period.

RT-PCR analysis demonstrated that the expression of *Fgf10* peaked on day 2 of culture and that its expression was maintained until day 10. *Sox9* showed a similar expression pattern to *Fgf10*, although its expression had been downregulated by day 10. *Col2a1* expression gradually increased throughout the culture period (Fig. 2M).

Overexpression of Fgf10 induced spiral deformation of Meckel's cartilage on the transfected side

First, protein production from the FGF10 expression vector was confirmed by Western blotting (Fig. 3A). The FGF10 protein was

detected in the culture supernatant collected from the transfected COS-7 cells, but not in the cell lysates of the transfected COS-7 cells or non-transfected samples.

Next, overexpression of *Fgf10* in the mandibular process was confirmed on the transfected side of the mandibular organ culture using RT-PCR analysis (Fig. 3B) and whole mount *in situ* hybridization (Fig. 3C) at 1 day after transfection. RT-PCR analysis demonstrated endogenous expression of the *Fgf10* gene on the non-transfected control side. However, RT-PCR analysis also showed higher expression of *Fgf10* on the transfected side than on the control side. Whole mount *in situ* hybridization analysis demonstrated localized ectopic

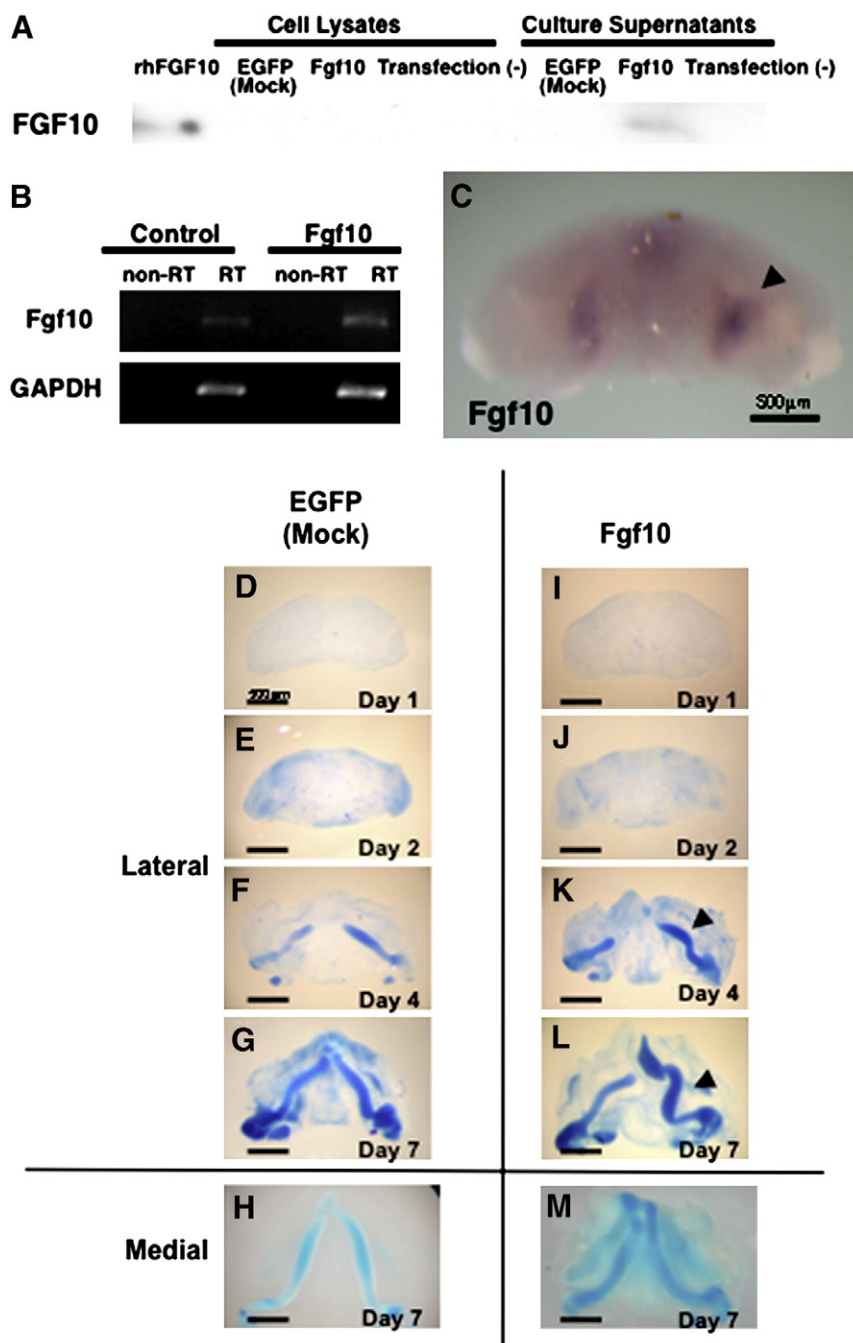


Fig. 3. Overexpression of the *Fgf10* gene and the formation of Meckel's cartilage. Protein production of FGF10 was detected in the culture media of the transfected COS-7 cells by Western blotting (A). Gene expression of *Fgf10* on the transfected and control sides of the mandible was analyzed by RT-PCR (B) and *in situ* hybridization analysis (C). *In situ* hybridization analysis showed increased but restricted gene expression of *Fgf10* (arrowhead). (D–N) Effects of *Fgf10* overexpression on Meckel's cartilage formation. Microphotographs of mandibles transfected with the *EGFP* or *Fgf10* gene, cultured for 0 to 7 days, and stained with Alcian blue are shown. Mandibular explants transfected with *EGFP* (D–H) or *Fgf10* (I–M) in the lateral (D–G, I–L) and medial region (H and M). An irregular and asymmetric rod-shaped piece of Meckel's cartilage was formed when *Fgf10* was transfected into the lateral region of the mandibular explants. Note the deformation of Meckel's cartilage (arrowhead). Bars = 500 μm.

expression of the transfected *Fgf10* (Fig. 3C; arrowhead on the right side) and weak endogenous expression of *Fgf10* (Fig. 3C; left side).

After being transfected with the *Fgf10* gene, the mandibular explants were stained with whole mount Alcian blue staining to elucidate the process of cartilage formation (Figs. 3, D–M). Meckel's cartilage was first found on day 3 and elongated in the anterior and posterior directions on day 4 (Fig. 3F). The cartilage in the explants transfected with mock vector in the lateral or medial regions grew symmetrically, and V-shaped rods with small masses had formed at the posterior end by day 7 (Figs. 3G and H). Beside the lateral rod of Meckel's cartilage, a mass of secondary cartilage, which would be a mandibular condylar cartilage and/or gonial angle cartilage formed (Fig. 3G). In contrast, an irregularly deformed rod-shaped piece of Meckel's cartilage with a spiral shape was formed when *Fgf10* was transfected into the lateral region of the mandibular explants (Fig. 3K). This asymmetry continued until the end of the culture period (Fig. 3L). The secondary cartilages were also deformed along the Meckel's cartilage. Meanwhile, medially transfected *Fgf10* did not induce Meckel's cartilage deformation in the mandibular explant (Fig. 3M).

Overexpression of Fgf10 induced the elongation of Meckel's cartilage and the gene expression of chondrogenic markers

We further analyzed the deformation of Meckel's cartilage quantitatively at 7 days after the overexpression of *Fgf10*. While 6 of 38 explants showed a partial non-spiral asymmetric shape in the control groups which was limited in the experimental variation, apparent spiral deformation was found after the overexpression of *Fgf10* in 20 of 27 explants in the lateral region and 2 of 9 explants in the medial region showed non-spiral partial asymmetry (Table 2).

In order to precisely understand the morphological changes of the cartilage, we reconstructed Meckel's cartilage three dimensionally (Figs. 4A–D) and measured the three-dimensional topographic length of the long axis (Figs. 4, G and H). No difference was observed between the transfected and non-transfected side when EGFP was delivered to the lateral region of the mandible (Fig. 4G). On the other hand, the topographic length of the long axis on the side transfected with *Fgf10* was significantly longer than that on the control side (Fig. 4G, $N=5$, $p<0.05$). Conversely, there were no significant differences in the length of the cartilage between the transfected and non-transfected side when EGFP or *Fgf10* was delivered to the medial region of the mandible (Fig. 4H, $N=5$).

When *Fgf10* gene was transfected to the lateral region of the mandible, H&E staining of tissue sections of the samples at day 7 after *Fgf10* transfection showed the deformation of the Meckel's cartilage and cartilage-like structure at the out-lateral side of the Meckel's cartilage (Fig. 4I). *In situ* hybridization analysis of the tissue sections showed that the cells in the deformed cartilage tissues expressed a chondrocyte marker such as *Col2a1* (Fig. 4J) at 7 days after *Fgf10* transfection. On the other hand, H&E staining of tissue sections didn't show the deformation of the cartilage (Fig. 4K), and the expression pattern of *Col2a1* was normal (Fig. 4L) when *Fgf10* gene was transfected to the medial region.

To investigate the regulation of genes related to chondrogenesis by *Fgf10* quantitatively, we extracted RNA from the mandibular explant

cultures on days 1–7. Semi-quantitative RT-PCR analysis showed that the expression of *Sox9* was significantly increased on day 4 on the *Fgf10* transfected side of the mandibular explant compared with the control side (Fig. 4M, $N=3$, triplicate, $p<0.05$). This upregulation was decreased on day 7 ($p<0.05$), and the expression level of *Sox9* was not significantly different between the two groups. The expression of *Col2a1* occurred at a similar level during the first 4 days of culture. However, it was significantly enhanced on day 7 shortly after the peak in *Sox9* expression (Fig. 4N, $N=3$, triplicate, $p<0.01$).

Time- and region-specific effects of FGF10 on chondrogenesis in mandibular micromass culture through the phosphorylation of ERK signaling

We examined the effect of recombinant human FGF10 (rhFGF10) treatment on the accumulation of cartilage matrix proteoglycans in mandibular micromass culture. Rat medial or lateral mandibular cell micromass culture was carried out in the presence or absence of rhFGF10. After 3 days of culture with rhFGF10, we divided the rhFGF10 treated groups into two groups based on whether the samples were further cultured with or without rhFGF10, which we designated (++) and (+–), respectively, as shown in Fig. 5. Representative data from the experimental groups (5 ng/ml rhFGF10) and control group are shown in Figs. 5A–F. Many Alcian blue-positive nodules formed in the mandibular cells derived from the lateral region (Figs. 5A–C); however, no nodule formation was observed in the cells from the medial region regardless of the presence or absence of rhFGF10 (Figs. 5D–F). Measurement of the Alcian blue-positive area demonstrated a significant increase in size when rhFGF10 was added to the mandibular cells derived from the lateral region (Fig. 5G, $p<0.01$) compared with the areas observed in both groups of cells derived from the medial region. rhFGF10 promoted the formation of cartilage from the lateral mandibular cells at 5 ng/ml (Figs. 5G and H, $p<0.05$). FGF stimulation in the first 3 days of culture induced the chondrogenic nodule formation of cells derived from lateral region, but not further stimulated in prolonged application. No significant difference in cartilage nodule formation was found between the two medial groups at any concentration.

The addition of 5 or 25 ng/ml FGF10 to the mandibular micromass cultures caused a significant increase in extracellular signal-regulated kinase-1 (ERK-1) phosphorylation in the cells from the lateral region (Fig. 5I, $p<0.05$).

FGF10 had no effect on cell proliferation in the mandibular cell culture

We examined the effect of rhFGF10 on cell proliferation in a monolayered mandibular cell culture system, and we regarded the absorbance at 0 ng of FGF10 protein as 100%. rhFGF10 treatment did not affect the number of cells from the lateral region of the mandibular process in the mandibular cell culture system (Fig. 5J). Moreover, the incorporation of BrdU was not affected by rhFGF10 protein application to the mandibular cells from the lateral region (data not shown).

Discussion

Roles of FGF10 signaling during the formation of Meckel's cartilage

In the present study, it was demonstrated for the first time, that the region in which *Sox9* and *Col2a1* were expressed was adjacent to the area where *Fgf10* mRNA expression was detected. The expression domain demonstrating *Sox9* and *Col2a1* expression at E12 formed Meckel's cartilage thereafter. While the expression domains of the FGFR were not so clearly localized, all of the FGFR expressed in the mandibular mesenchyme have the potential to be mediators of FGF signaling during Meckel's cartilage development. Quantitatively, the

Table 2
Asymmetric rate of Meckel's cartilage formation.

| | Asymmetric rate | |
|----------------------|-----------------|-----|
| EGFP (mock) lateral | 4/20 | 20% |
| <i>Fgf10</i> lateral | 20/27 | 74% |
| EGFP (mock) medial | 0/5 | 0% |
| <i>Fgf10</i> medial | 2/9 | 22% |

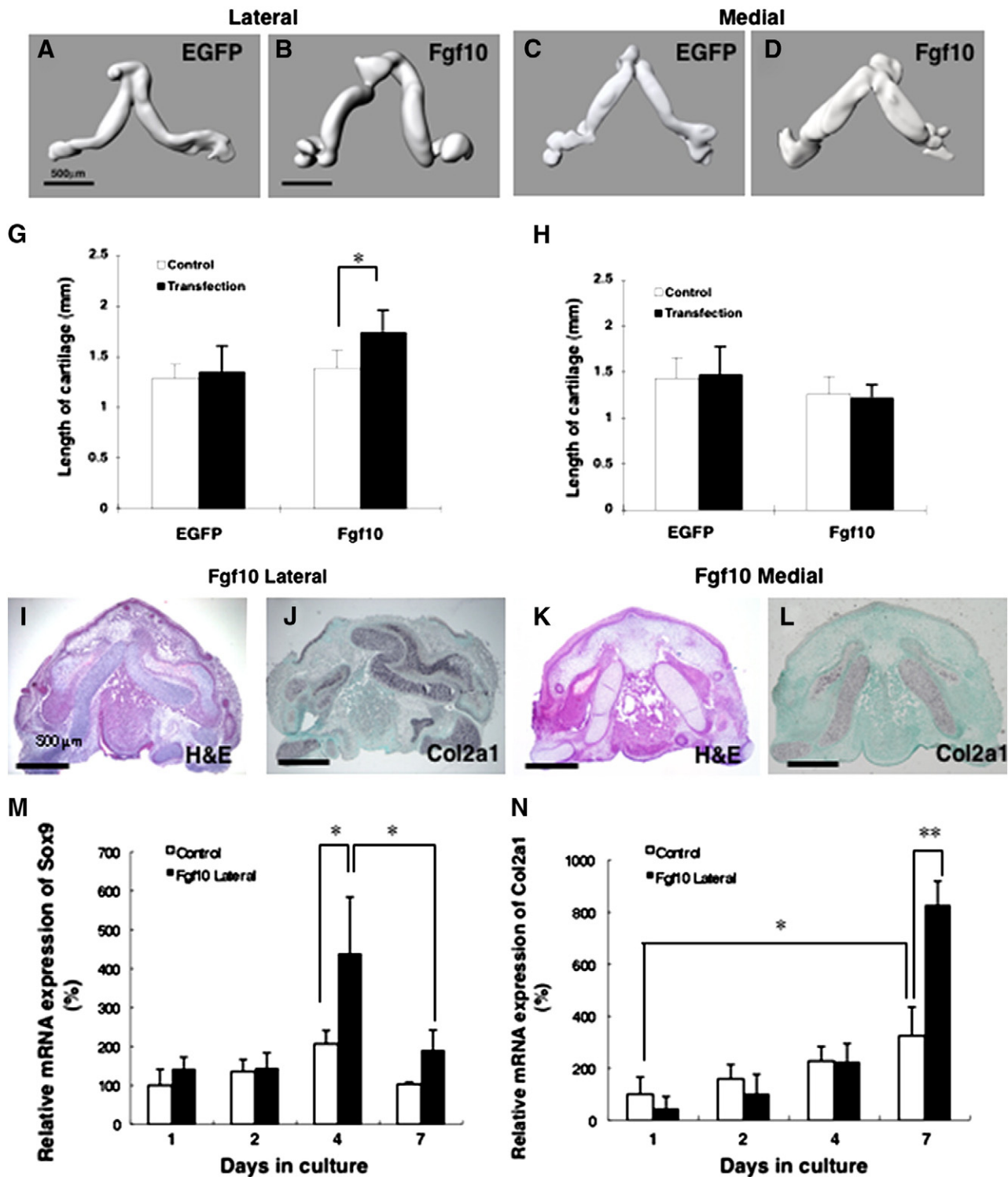


Fig. 4. Three-dimensional topographical analysis of Meckel's cartilage and the effects of *Fgf10* overexpression on the expression of chondrogenic marker genes. (A–D) 3D reconstructed image of Meckel's cartilage. Stereological analysis demonstrated that Meckel's cartilage was spirally deformed in the FGF10 overexpressed sample in the lateral region (B). (G and H) Representative graphs of cartilage rod length on the gene-transfected and control sides. The results are expressed as the mean \pm SD (*: $p < 0.05$, $N = 5$ in each group). The cartilage length on the side transfected with *Fgf10* in the lateral region was significantly longer than that on the control side (D). (I–L) H&E staining and *in situ* hybridization of tissue sections from the mandibular explant at 7 days after *Fgf10* transfection. H&E staining (I and K), *Col2a1* (J and L). (M and N) Representative graphs of the expression levels of *Sox9* and *Col2a1* mRNA according to semi-quantitative RT-PCR. (M) A significant increase in *Sox9* expression on the treated side compared with the control side was demonstrated at day 4 after transfection (*: $p < 0.05$, $N = 3$ in each group). At day 4, *Sox9* expression on the treated side was significantly increased during the culture period (*: $p < 0.05$). (N) Gene expression of *Col2a1* on the treated and control sides (*: $p < 0.05$, **: $p < 0.01$). A significant increase in *Col2a1* expression on the treated side compared with the control side was demonstrated at day 7 after transfection (**: $p < 0.01$, $N = 3$ in each group).

expression of *Fgf10* and *Sox9* peaked on day 2 and day 4 of culture, respectively, while *Col2a1* expression increased from day 4 and maintained its expression level until day 10 during the formation of

Meckel's cartilage. These results suggested that FGF10 is spatially associated with gene regulation in the development of Meckel's cartilage.

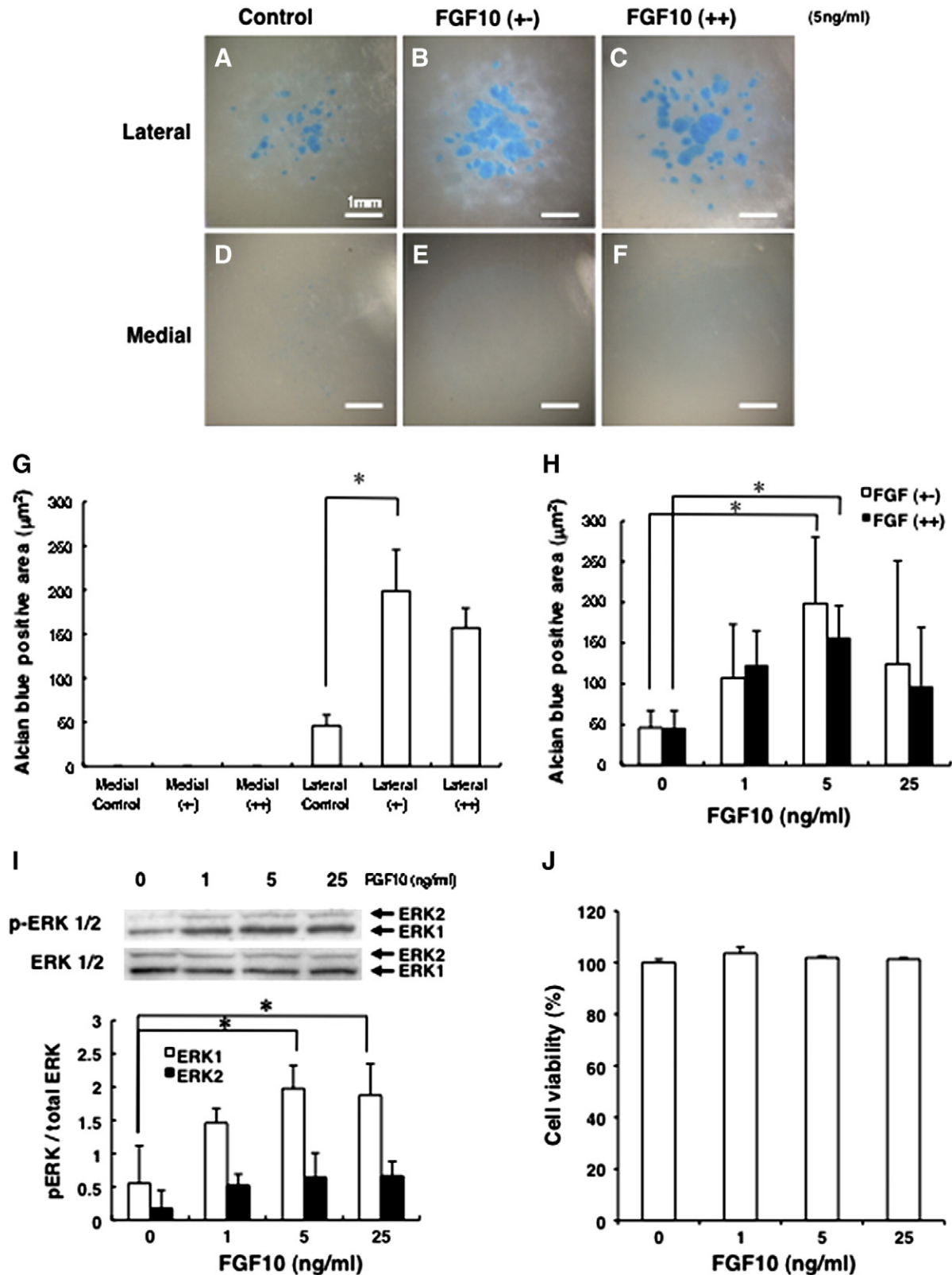


Fig. 5. Effects of FGF10 protein on the production of cartilage matrix proteoglycans and ERK phosphorylation in micromass cultures of mandibular cells. (A–F) Micromass cultures stained with Alcian blue. Cells derived from the lateral (A–C) and medial regions (D–F) are shown. (G) Representative graphs of position-dependent and time dependent differences in the Alcian blue positive nodule area induced by treatment with rhFGF10 (5 ng/ml). Note that treatment with 5 ng/ml FGF10 increased Alcian blue-stained nodule formation in the lateral region of the mandibular cell culture. Continuous treatment with rhFGF10 (++) did not alter the positive area compared to the samples treated with rhFGF10 alone for the first 3 days (+-). (H) Dose-dependent effect of rhFGF10 on the Alcian blue-positive area in the mandibular micromass culture. rhFGF10 treatment significantly increased the Alcian blue-positive area at 5 ng/ml. Each column represents the mean area \pm SD (N = 3 in each group). (I) Western blot analysis of ERK phosphorylation in the mandibular micromass culture system. a) Treatment with FGF10 increased the phosphorylation of ERK at 1 day of culture. b) Representative graphs of the band density. The phosphorylation of ERK1 was significantly increased by FGF10 treatment at 5 ng/ml and 25 ng/ml compared to the control (0 ng/ml), but the phosphorylation of ERK2 was unchanged. Each column represents the mean \pm SD (*: $p < 0.05$, N = 3 in each group). (J) Effect of rhFGF10 treatment on cell proliferation in the mandibular cell micromass culture. Cell proliferation was not altered at any concentration of FGF10 treatment ($p = 0.45$). (++) : Samples supplemented with rhFGF10 protein throughout the experimental period, and (+-) : samples supplemented with rhFGF10 alone for the first 3 day.

There have been several studies during mandibular morphogenesis in early development. Shum et al. demonstrated the similar phenotypic change by EGF abrogation in mandibular organ culture system (Shum et al., 1993). Nonaka et al. indicated that the BMP-soaked bead induced ectopic chondrogenesis was inhibited by the application of EGF. Thus, EGF and its downstream of tyrosine kinase pathway could inhibit chondrogenesis and regulate the shape of the Meckel's cartilage. While FGF also shares downstream tyrosine kinase pathway with EGF, since increased activity of FGF signaling pathway induced shape change in Meckel's cartilage as shown in the present study, FGF could interfere or affect the EGF signaling to regulate the size and shape of Meckel's cartilage. In addition, it is known that the epithelial–mesenchymal interaction plays an important role in mandibular development (Mina et al., 1994). A recent study in which *Fgf8* expression was abrogated in the epithelium of the mandibular process using Cre-loxP technology revealed that FGF8 is necessary for normal development and morphogenesis of the lateral regions of the developing mandible involved in the formation of Meckel's cartilage (Trumpp et al., 1999). Mesenchymal expression of *Fgf10* and neural crest survival was found to be decreased in *Fgf8* hypomorphic mutant mice (Frank et al., 2002). These data implied that FGF10 plays a role in mandibular morphogenesis in association with FGF8 under the control of epithelial–mesenchymal interactions.

On the other hand, *Fgf10* knockout mice did not show any severe abnormalities during mandibular morphogenesis (Min et al., 1998; Sekine et al., 1999), even though they exhibited cleft palates and died at birth because of a lack of lung development (Rice et al., 2004). In addition, FGFR2b, one of the major receptors for FGF10 (Ornitz et al., 1996), null mice had thinner mandibles and showed severe defects of the limbs and lung as well as abnormalities in the craniofacial region (De Moerloose et al., 2000). It was suspected that other FGF expressed in the mandibular mesenchyme compensate for the loss of FGF10 in *FGF10* knockout mice through *Fgfr2b* signaling (Alvarez et al., 2003; Kettunen et al., 2000). Since *Fgfr2* was expressed in the mandible, it is possible that the phenotypic effects shown in the present study were expressed through the FGF10–FGFR2 signaling pathway. In a previous study of mandibular chondrogenesis, the expression of dominant-negative FGFR3 in the developing chick mandible resulted in the truncation of Meckel's cartilage and severely reduced outgrowth of the mandibular process (Mina and Havens, 2007). The opposite phenotype shown in the present study could be interpreted as demonstrating that FGF10–FGFR3 signaling also regulates Meckel's cartilage development.

Interestingly, our results suggested that FGF10 affected the formation of secondary cartilage at the outer side of the Meckel's cartilage. It could be considered as the anlage of mandibular condylar cartilage and/or gonial angle cartilage characteristically seen in the rodents. It is generally known to form in the later stages of mandibular development. Apparently, along with Meckel's cartilage, it showed asymmetric deformation. While previous studies have also shown this cartilage in mandibular organ culture system (Shum L, et al., 19–), information available is very limited. To identify the cartilage and to analyze the functional roles of FGF10 on their development, further investigations are needed.

Taken together, when FGF10 signaling is downregulated, the pathway could be compensated for by other FGF; however, as shown in the present study, overexpression of FGF10 had a specific effect on Meckel's cartilage formation, which was mediated through the FGFR2 or FGFR3 pathway.

FGF10 did not enhance the proliferation of mandibular cells in the lateral region

In this study, we achieved the overexpression of *Fgf10* in an area where endogenous *Fgf10* expression was detected (Fig. 3). This increased the length of Meckel's cartilage on the lateral side of the mandible and the expression levels of chondrogenic markers. We

hypothesized that the increase in cell proliferation enhanced chondrogenesis in the mandibular explant. However, FGF10 protein affected neither DNA synthesis nor cell proliferation in the mandibular culture according to the BrdU incorporation assay and cell proliferation assay. Meanwhile, our histological observations did not indicate any cytological alterations in Meckel's cartilage. In addition, while the size of Meckel's cartilage was affected, the overall size of the explants was not changed. Thus, it could be considered that FGF10 mainly influenced chondrocyte differentiation in the present study. Therefore, the changes observed in the size and shape of Meckel's cartilage may have been caused by the recruitment of undifferentiated mesenchymal cells to the chondrocyte lineage.

Position- and time-dependent roles of FGF10 during mandibular morphogenesis

Although FGF10 induced phenotypic changes when it was overexpressed on the lateral side, no effects were found in the medial area at E12.5. In addition, cells derived from the medial section of the mandibular prominences did not respond to FGF10 application in the micromass culture experiments. This position-dependent change may have occurred as a result of cellular differences between the lateral and medial areas shown by difference in expression of *Fgfr1* and *Fgfr2* in the present study. In a previous study, BMP4 induced ectopic cartilage formation when it was applied inside Meckel's cartilage, but did not when applied to the lateral side (Nonaka et al., 1999; Semba et al., 2000). Meanwhile, phenotypic evaluation of Cre-loxP mutant mice provided evidence that FGF8 signaling plays essential roles in mandibular morphogenesis in the lateral region (Trumpp et al., 1999). These studies showed the different responses of FGF between the lateral and medial regions of the mandible. Since the differentiation of chondrocytes began from the lateral region of the mandible and extended to the medial and posterior areas (Bhaskar et al., 1953), cells may be most susceptible to FGF10 stimulation immediately before chondrogenic differentiation.

Since the positive regulatory effects on chondrogenesis were produced by the application of FGF10 in the earlier half of the mandibular micromass culture, it could be considered that stimulation with FGF10 acts in a time dependent manner. In addition, our preliminary experiments suggested that the overexpression of *Fgf10* at E13.5 in the mandibular organ culture did not affect the shape of Meckel's cartilage (data not shown). These results implied that FGF10 affects the early stages of cartilage formation. It has been known in general that the CNCC migrates to the facial primordia prior to the formation of mandibular prominence and develops to various organs in the first and second branchial arch around E11 to E13 in rats. Short-term earlier stimulation by FGF10 in the present study was placed in this time window. Therefore, it could be considered that stimulation by FGF10 was needed and to be enough to enhance the chondrogenic differentiation in this process of differentiation.

Taken together, we found that the recruitment of mesenchymal cells to a chondrogenic lineage by FGF10 during Meckel's cartilage formation was precisely controlled in a time and position dependent manner.

FGF10 signaling stimulates chondrogenic differentiation through ERK phosphorylation

Since our results indicated that an increased size of Meckel's cartilage was produced by FGF10 overexpression, it could be considered that the differentiation of chondrocytes was altered by the overexpression of FGF10 in the lateral region of the mandible. Meanwhile, there was no apparent change in chondrogenesis when *Fgf10* gene was transfected to the forelimb mesenchyme at E12 rat (data not shown). These data suggest that the function of *Fgf10* in limb development is different from that in mandibular development.

It was reported that frontonasal-derived mesenchymal cells and mandible-derived chondrocytes showed opposite responses to FGF; i.e., the differentiation of the mandibular mesenchyme was positively enhanced, while that of the frontonasal mesenchyme was not (Bobick et al., 2006) under the control of ERK activation. Our results indicated that FGF10 treatment induced increased phosphorylation of ERK1 in embryonic mandibular cells. Thus, FGF10 signaling may be mediated by the MEK/ERK pathway and cause enhanced chondrogenic differentiation during Meckel's cartilage formation.

Conclusion

FGF10 enhanced chondrogenic differentiation in the mandibular mesenchyme and increases the length of Meckel's cartilage through FGF10/FGFR signaling cascade. FGFR3 and FGFR2 are the candidates for the receptor for this stimulation and further investigations are needed to specify the pathway. In conclusion, FGF10 regulates the size and shape of Meckel's cartilage during mandibular morphogenesis time- and position-dependently through the MEK/ERK signal transduction pathway.

Acknowledgments

This work was funded by: Ministry of Education, Culture, Sports, Science and Technology, Japan, Takeda Science Foundation, Japan and Tohoku University Interface Oral Health Science, Japan.

References

- Alvarez, Y., Alonso, M.T., Vendrell, V., Zelarayan, L.C., Chamero, P., Theil, T., Bösl, M.R., Kato, S., Maconochie, M., Riethmacher, D., Schimmang, T., 2003. Requirements for FGF3 and FGF10 during inner ear formation. *Development* 130, 6329–6338.
- Bhaskar, S.N., Weinmann, J.P., Schour, I., 1953. Role of Meckel's cartilage in the development and growth of the rat mandible. *J. Dent. Res.* 32, 398–410.
- Bi, W., Deng, J.M., Zhang, Z., Behringer, R.R., de Crombrughe, B., 1999. Sox9 is required for cartilage formation. *Nat. Genet.* 22, 85–89.
- Bobick, B.E., Thornhill, T.M., Kulyk, W.M., 2006. Fibroblast growth factors 2, 4, and 8 exert both negative and positive effects on limb, frontonasal, and mandibular chondrogenesis via MEK–ERK activation. *J. Cell. Physiol.* 211, 233–243.
- Chai, Y., Bringas, P., Shuler, C., Devaney, E., Grosschedl, R., Slavkin, H.C., 1998. A mouse mandibular culture model permits the study of neural crest cell migration and tooth development. *Int. J. Dev. Biol.* 42, 87–94.
- Chai, Y., Jiang, X., Ito, Y., Bringas Jr., P., Han, J., Rowitch, D.H., Soriano, P., McMahon, A.P., Sucov, H.M., 2000. Fate of the mammalian cranial neural crest during tooth and mandibular morphogenesis. *Development* 127, 1671–1679.
- Cobourne, M.T., Sharpe, P.T., 2003. Tooth and jaw: molecular mechanisms of patterning in the first branchial arch. *Arch. Oral Biol.* 48, 1–14.
- De Moerloose, L., Spencer-Dene, B., Revest, J.M., Hajihosseini, M., Rosewell, I., Dickson, C., 2000. An important role for the IIIb isoform of fibroblast growth factor receptor 2 (FGFR2) in mesenchymal–epithelial signalling during mouse organogenesis. *Development* 127, 483–492.
- Ferguson, C.A., Tucker, A.S., Sharpe, P.T., 2000. Temporospatial cell interactions regulating mandibular and maxillary arch patterning. *Development* 127, 403–412.
- Frank, D.U., Fotheringham, L.K., Brewer, J.A., Muglia, L.J., Tristani-Firouzi, M., Capocchi, M.R., Moon, A.M., 2002. An Fgf8 mouse mutant phenocopies human 22q11 deletion syndrome. *Development* 129, 4591–4603.
- Havens, B.A., Rodgers, B., Mina, M., 2006. Tissue-specific expression of Fgfr2b and Fgfr2c isoforms, Fgf10 and Fgf9 in the developing chick mandible. *Arch. Oral Biol.* 51, 134–145.
- Kettunen, P., Laurikkala, J., Itäranta, P., Vainio, S., Itoh, N., Thesleff, I., 2000. Associations of FGF-3 and FGF-10 with signaling networks regulating tooth morphogenesis. *Dev. Dyn.* 219, 322–332.
- Lewandoski, M., Sun, X., Martin, G.R., 2000. Fgf8 signalling from the AER is essential for normal limb development. *Nat. Genet.* 26, 460–463.
- Min, H., Danilenko, D.M., Scully, S.A., Bolon, B., Ring, B.D., Tarpley, J.E., DeRose, M., Simonet, W.S., 1998. Fgf-10 is required for both limb and lung development and exhibits striking functional similarity to *Drosophila* branchless. *Genes Dev.* 12, 3156–3161.
- Mina, M., 2001. Morphogenesis of the medial region of the developing mandible is regulated by multiple signaling pathways. *Cells Tissues Organs* 169, 295–301.
- Mina, M., Havens, B., 2007. FGF signaling in mandibular skeletogenesis. *Orthod. Craniofac. Res.* 10, 59–66.
- Mina, M., Upholt, W.B., Kollar, E.J., 1994. Enhancement of avian mandibular chondrogenesis in vitro in the absence of epithelium. *Arch. Oral Biol.* 39, 551–562.
- Neubüser, A., Peters, H., Balling, R., Martin, G.R., 1997. Antagonistic interactions between FGF and BMP signaling pathways: a mechanism for positioning the sites of tooth formation. *Cell* 90, 247–255.
- Nonaka, K., Shum, L., Takahashi, I., Takahashi, K., Ikura, T., Dashner, R., Nuckolls, G.H., Slavkin, H.C., 1999. Convergence of the BMP and EGF signaling pathways on Smad1 in the regulation of chondrogenesis. *Int. J. Dev. Biol.* 43, 795–807.
- Ohtani, H., Kuroiwa, A., Obinata, M., Ooshima, A., Nagura, H., 1992. Identification of type I collagen-producing cells in human gastrointestinal carcinomas by non-radioactive in situ hybridization and immunoelectron microscopy. *J. Histochem. Cytochem.* 40, 1139–1146.
- Ohuchi, H., Nakagawa, T., Yamamoto, A., Araga, A., Ohata, T., Ishimaru, Y., Yoshioka, H., Kuwana, T., Nohno, T., Yamasaki, M., Itoh, N., Noji, S., 1997. The mesenchymal factor, FGF10, initiates and maintains the outgrowth of the chick limb bud through interaction with FGF8, an apical ectodermal factor. *Development* 124, 2235–2244.
- Ornitz, D.M., Xu, J., Colvin, J.S., McEwen, D.G., MacArthur, C.A., Coulier, F., Gao, G., Goldfarb, M., 1996. Receptor specificity of the fibroblast growth factor family. *J. Biol. Chem.* 271, 15292–15297.
- Rice, R., Spencer-Dene, B., Connor, E.C., Gritli-Linde, A., McMahon, A.P., Dickson, C., Thesleff, I., Rice, D.P., 2004. Disruption of Fgf10/Fgfr2b-coordinated epithelial–mesenchymal interactions causes cleft palate. *J. Clin. Invest.* 113, 1692–1700.
- Rosen, B., Beddington, R.S., 1993. Whole-mount in situ hybridization in the mouse embryo: gene expression in three dimensions. *Trends Genet.* 9, 162–167.
- Sasano, Y., Furusawa, M., Ohtani, H., Mizoguchi, I., Takahashi, I., Kagayama, M., 1996. Chondrocytes synthesize type I collagen and accumulate the protein in the matrix during development of rat tibial articular cartilage. *Anat. Embryol. (Berl.)* 194, 247–252.
- Sekine, K., Ohuchi, H., Fujiwara, M., Yamasaki, M., Yoshizawa, T., Sato, T., Yagishita, N., Matsui, D., Koga, Y., Itoh, N., Kato, S., 1999. Fgf10 is essential for limb and lung formation. *Nat. Genet.* 21, 138–141.
- Semba, I., Nonaka, K., Takahashi, I., Takahashi, K., Dashner, R., Shum, L., Nuckolls, G.H., Slavkin, H.C., 2000. Positionally-dependent chondrogenesis induced by BMP4 is co-regulated by Sox9 and Msx2. *Dev. Dyn.* 217, 401–414.
- Shigetani, Y., Nobusada, Y., Kuratani, S., 2000. Ectodermally derived FGF8 defines the maxillomandibular region in the early chick embryo: epithelial–mesenchymal interactions in the specification of the craniofacial ectomesenchyme. *Dev. Biol.* 228, 73–85.
- Shum, L., Sakakura, Y., Bringas, P., Luo, W., Snead, M.L., Mayo, M., Crohin, C., Millar, S., Werb, Z., Buckley, S., 1993. EGF abrogation-induced fusilli-form dysmorphogenesis of Meckel's cartilage during embryonic mouse mandibular morphogenesis in vitro. *Development* 118, 903–917.
- Silbermann, M., von der Mark, K., 1990. An immunohistochemical study of the distribution of matril proteins in the mandibular condyle of neonatal mice. I. Collagens. *J. Anat.* 170, 11–22.
- Slavkin, H.C., Sasano, Y., Kikunaga, S., Bessem, C., Bringas, P., Mayo, M.L., Luo, W., Mak, G., Rall, L., Snead, M.L., 1990. Cartilage, bone and tooth induction during early embryonic mouse mandibular morphogenesis using serumless, chemically-defined medium. *Connect. Tissue Res.* 24, 41–51.
- Steinberg, Z., Myers, C., Heim, V.M., Lathrop, C.A., Beustini, I.T., Stewart, J.S., Larsen, M., Hoffman, M.P., 2005. FGFR2b signaling regulates ex vivo submandibular gland epithelial cell proliferation and branching morphogenesis. *Development* 132, 1223–1234.
- Terao, F., Takahashi, I., Mitani, H., Haruyama, N., Suzuki, O., Sasano, Y., Takano-Yamamoto, T., 2007. Application of electroporation to mandibular explant culture system for gene transfection. *Interface Oral Health Sci.* 2007, 179–180.
- Trumpp, A., Depew, M.J., Rubenstein, J.L., Bishop, J.M., Martin, G.R., 1999. Cre-mediated gene inactivation demonstrates that FGF8 is required for cell survival and patterning of the first branchial arch. *Genes Dev.* 13, 3136–3148.
- Unbekandt, M., del Moral, P.M., Sala, F.G., Bellusci, S., Warburton, D., Fleury, V., 2008. Tracheal occlusion increases the rate of epithelial branching of embryonic mouse lung via the FGF10-FGFR2b-Sprouty2 pathway. *Mech. Dev.* 125, 314–324.
- Yamane, A., Amano, O., Slavkin, H.C., 2003. Insulin-like growth factors, hepatocyte growth factor and transforming growth factor- α in mouse tongue myogenesis. *Dev. Growth Differ.* 45, 1–6.
- Zhu, J.X., Sasano, Y., Takahashi, I., Mizoguchi, I., Kagayama, M., 2001. Temporal and spatial gene expression of major bone extracellular matrix molecules during embryonic mandibular osteogenesis in rats. *Histochem. J.* 33, 25–35.